

# Chemical Science

Accepted Manuscript



This is an *Accepted Manuscript*, which has been through the Royal Society of Chemistry peer review process and has been accepted for publication.

*Accepted Manuscripts* are published online shortly after acceptance, before technical editing, formatting and proof reading. Using this free service, authors can make their results available to the community, in citable form, before we publish the edited article. We will replace this *Accepted Manuscript* with the edited and formatted *Advance Article* as soon as it is available.

You can find more information about *Accepted Manuscripts* in the [Information for Authors](#).

Please note that technical editing may introduce minor changes to the text and/or graphics, which may alter content. The journal's standard [Terms & Conditions](#) and the [Ethical guidelines](#) still apply. In no event shall the Royal Society of Chemistry be held responsible for any errors or omissions in this *Accepted Manuscript* or any consequences arising from the use of any information it contains.

Cite this: DOI: 10.1039/coxx00000x

www.rsc.org/xxxxxx

ARTICLE TYPE

# Fe(IV) alkylidenes via protonation of Fe(II) vinyl chelates and a comparative Mössbauer spectroscopic study

Brian M. Lindley,<sup>a</sup> Ala'aeddeen Swidan,<sup>a</sup> Emil B. Lobkovsky,<sup>a</sup> Peter T. Wolczanski,<sup>a\*</sup> Mario Adelhardt, Jörg Sutter,<sup>b</sup> and Karsten Meyer<sup>b</sup>

<sup>5</sup> Received (in XXX, XXX) Xth XXXXXXXXX 20XX, Accepted Xth XXXXXXXXX 20XX  
DOI: 10.1039/b000000x

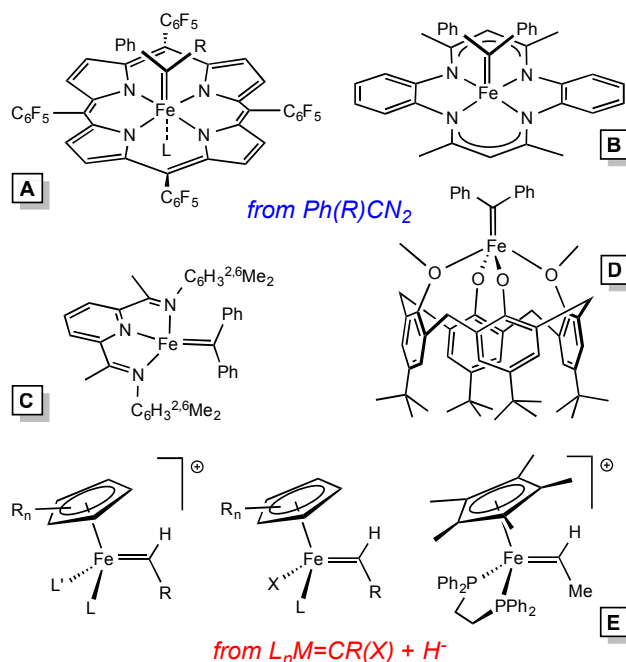
Treatment of *cis*-Me<sub>2</sub>Fe(PMe<sub>3</sub>)<sub>4</sub> with di-1,2-(*E*-2-(pyridin-2-yl)vinyl)benzene ((bdvp)H<sub>2</sub>), a tetradentate ligand precursor, afforded (bdvp)Fe(PMe<sub>3</sub>)<sub>2</sub> (1-PMe<sub>3</sub>) and 2 equiv CH<sub>4</sub>, via C-H bond activation. Similar treatments with tridentate ligand precursors PhCH=NCH<sub>2</sub>(*E*-CH=CHPh) ((pipp)H<sub>2</sub>) and PhCH=N(2-CCMe-Ph) ((pipa)H) under dinitrogen provided *trans*-(pipp)Fe(PMe<sub>3</sub>)<sub>2</sub>N<sub>2</sub> (2) and *trans*-(pipvd)Fe(PMe<sub>3</sub>)<sub>2</sub>N<sub>2</sub> (3), respectively, the latter via one C-H bond activation, and a subsequent insertion of the alkyne into the remaining Fe-Me bond. All three Fe(II) vinyl species were protonated with H[BAr<sup>F</sup><sub>4</sub>] to form the corresponding Fe(IV) alkylidene cations, [(bavp)Fe(PMe<sub>3</sub>)<sub>2</sub>][BAr<sup>F</sup><sub>4</sub>] (4-PMe<sub>3</sub>), [(piap)Fe(PMe<sub>3</sub>)<sub>3</sub>][BAr<sup>F</sup><sub>4</sub>] (5), and [(pipad)Fe(PMe<sub>3</sub>)<sub>3</sub>][BAr<sup>F</sup><sub>4</sub>] (6). Mössbauer spectroscopic measurements on the formally Fe(II) and Fe(IV) derivatives revealed isomer shifts within 0.1 mm/s, reflecting the similarity in their bond distances.

## Introduction

Homogeneous alkylidene compounds that catalyze olefin metathesis<sup>1-5</sup> typically contain 2nd row transition metals that have modest limitations regarding functionality tolerance (e.g., Mo),<sup>1,2</sup> and relative abundance (e.g., Ru).<sup>3,4</sup> Applications to commodity chemicals production have been hampered by these factors, and inexpensive first row transition metal alternatives hold great promise in solving some of the problems. Thus far, the synthesis of 1st row transition metal alkylidene complexes has presented a significant challenge to the organometallic community, especially in the case of iron.

Electronic structure analysis by Hoffmann *et al.*<sup>6</sup> suggests that metathesis catalysts need to be d<sup>n</sup> (n ≤ 4), hence Fe(IV) alkylidenes are the target of interest, especially in analogy to their 2nd row congeners. Several Fe(IV) alkylidenes have been synthesized, with two routes utilized in the cases of those structurally characterized (Fig. 1): 1) conversion of [CpLL'Fe=C(OR)R']<sup>+</sup> via hydride or alkyl anion reagents,<sup>7-9</sup> and 2) the addition of diazoalkanes, typically Ph<sub>2</sub>CN<sub>2</sub>, to coordinatively unsaturated complexes or labile precursors.<sup>10-13</sup> The subsequent chemistry has been limited to carbene transfers, and some transformations that hint at radical reactions.

In an effort to expand the scope of Fe(IV) alkylidenes, and to develop new synthetic paths, Fe(II) vinyl chelates have been explored as potential precursors to cationic Fe(IV) alkylidenes via protonation.<sup>14-18</sup> Entry into ferrous vinyl derivatives was implemented via precedented C-H bond activations by Karsch's *cis*-Me<sub>2</sub>Fe(PMe<sub>3</sub>)<sub>4</sub><sup>19</sup> complex.<sup>20-23</sup> While viable olefin metathesis catalysts containing Fe have not yet been realized, the generality of this approach suggests that incremental advances may yet prove successful.

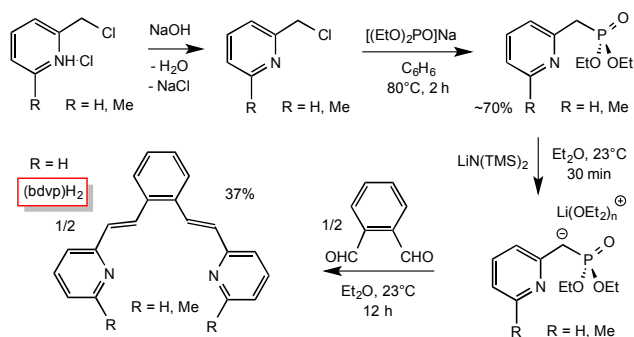


<sup>50</sup> Fig. 1 Some iron alkylidenes and methods of synthesis.

## Results and Discussion

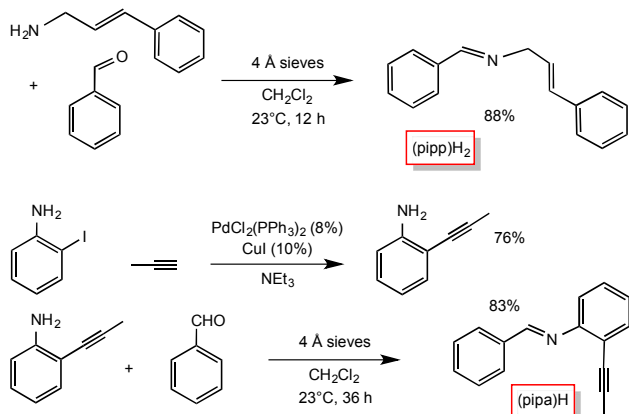
### Di-1,2-(*E*-2-(pyridin-2-yl)vinyl)benzene: Tetradentate Ligand Precursor

<sup>55</sup> As Scheme 1 illustrates, incorporation of two vinyl groups into a tetradentate chelate precursor was predicated on successful



**Scheme 1** Preparation of divinyl ligand precursor, 1,2-(*E*-2-(pyridin-2-yl)vinyl)benzene ((bdvp) $H_2$ ).

implementation of a Horner-Wadsworth-Emmons reaction to achieve the requisite *E*-stereochemistry. The modified 2-pyridylmethyl reagent was prepared according to a literature procedure<sup>24</sup> from  $Na[OP(OEt)_2]$  and 2-pyridylmethylchloride in 70% yield. Its addition to 1,2-benzene-dialdehyde afforded di-1,2-(*E*-2-(pyridin-2-yl)vinyl)benzene ((bdvp) $H_2$ , *E/Z* > 19:1) in 37% yield upon crystallization from ether/hexane.



**Scheme 2** Preparation of tridentate precursors,  $PhCH=NCH_2(E-CH=CHPh)$  ((pipp) $H_2$ ) and  $PhCH=N(2-CCMe-Ph)$  ((pipa) $H$ ).

### Tridentate Ligand Precursors: $PhCH=NCH_2(E-CH=CHPh)$ and $PhCH=N(2-CCMe-Ph)$

Condensation routes afforded the two additional tridentate ligands used in this study, as shown in Scheme 2. Cinnamyl amine<sup>25</sup> and benzaldehyde were used to synthesize  $PhCH=NCH_2(E-CH=CHPh)$  ((pipp) $H_2$ ),<sup>26</sup> while 2-propynylaniline, prepared from Pd-catalyzed cross-coupling<sup>27</sup> of propyne and 2-iodo-aniline, and benzaldehyde were used to generate  $PhCH=N(2-CCMe-Ph)$  ((pipa) $H$ ). A number of other potential imine and pyridine-containing tridentate ligand precursors were similarly made, but the subsequent C-H bond activations proved to be too slow or ineffective, allowing for competitive  $cis-Me_2Fe(PMe_3)_4$  degradation.

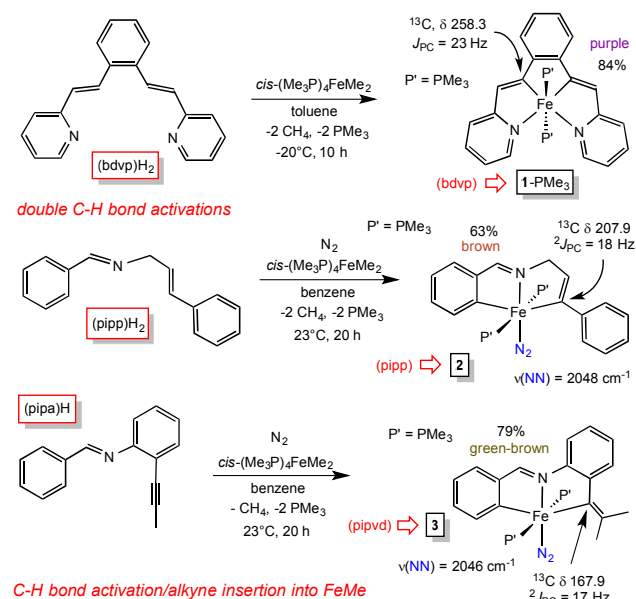
### Metalation via C-H Bond Activation and Insertion

Treatment of  $cis-Me_2Fe(PMe_3)_4$ <sup>19</sup> with tridentate precursor 1,2-(*E*-2-(pyridin-2-yl)vinyl)benzene ((bdvp) $H_2$ ) was undertaken at  $-20^\circ C$  in toluene. After 10 h, the solution was warmed to  $23^\circ C$  and concentrated to afford (bdvp) $Fe(PMe_3)_2$  (**1- $PMe_3$** ) in 84% yield as purple microcrystals (Scheme 3). The reaction is quite

sensitive to steric bulk, as use of a precursor possessing *o*-Me groups on the pyridines (Scheme 1) failed to metalate, and decomposition of  $cis-Me_2Fe(PMe_3)_4$  was instead observed.

A similar exposure of  $cis-Me_2Fe(PMe_3)_4$ <sup>19</sup> to  $PhCH=NCH_2(E-CH=CHPh)$  ((pipp) $H_2$ ) in benzene at  $23^\circ C$  after 20 h afforded a purple solid upon subsequent concentration (Scheme 3). Dissolution in THF under a dinitrogen atmosphere provided brown  $trans-(pipp)Fe(PMe_3)_2N_2$  (**2**) in 63% yield after removal of solvent. It is likely that the *tris*- $PMe_3$  derivative is formed initially, but  $N_2$  replaces  $PMe_3$  in a probable dissociative process. Previous examples have shown that steric factors -- in this case the phenyl substituent -- labilize the phosphine opposite the imine.<sup>23</sup> The dinitrogen ligand is readily discerned via its IR spectrum, which reveals a  $\nu(NN)$  at  $2048\text{ cm}^{-1}$ .<sup>28,29</sup>

A third, different metalation was conducted with  $PhCH=N(2-CCMe-Ph)$  ((pipa) $H$ ) and  $cis-Me_2Fe(PMe_3)_4$ . The precedented imine-directed Ar-H activation occurred, followed by insertion of



**Scheme 3** Methods employed in synthesizing vinyl precursors derived from CH-bond activation/metalation of  $cis-Me_2Fe(PMe_3)_4$  and acetylene insertion.

the pendant acetylene into the Fe-Me bond. The resulting complex,  $trans-(pipvd)Fe(PMe_3)_2N_2$  (**3**), contains a dimethylvinyl group as the precursor to a potential alkylidene. Green-brown **3** was prepared in 79% yield after metalation for 20 h at  $23^\circ C$ , and as in the previous case, it is likely an initially formed *tris*- $PMe_3$  complex lost a phosphine in the presence of  $N_2$  to afford the dinitrogen complex,<sup>23</sup> whose  $\nu(NN)$  is at  $2046\text{ cm}^{-1}$ .

All three precursors feature downfield  $^{13}C$  chemical shifts for the vinyl carbons bound to iron. A triplet ( $J_{PC} = 23\text{ Hz}$ ) corresponding to the Fe-C(Ar)= unit in (bdvp) $Fe(PMe_3)_2$  (**1- $PMe_3$** ) was located at  $\delta 258.3$ , an unusual shift that may be intrinsic to the metrics of its tridentate chelation, i.e., reflecting a very short d(Fe-C). The Fe-vinyl carbon of the trident chelate in  $trans-(pipp)Fe(PMe_3)_2N_2$  (**2**) also manifests a significant downfield shift at  $\delta 207.9$  (t,  $J_{PC} = 18\text{ Hz}$ ), while the Fe-C(Ar)= carbon of  $trans-(pipvd)Fe(PMe_3)_2N_2$  (**3**), the most sterically hindered vinyl, resonates at  $\delta 167.9$  (t,  $J_{PC} = 17\text{ Hz}$ ).

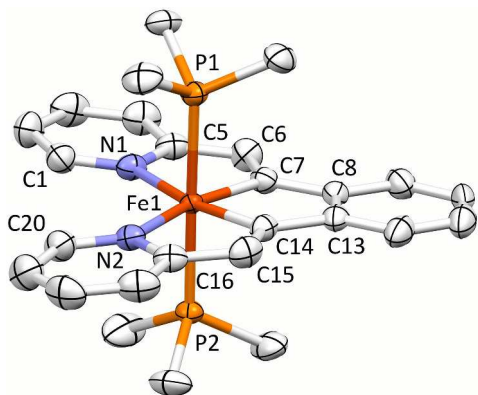


**Fig. 2** Molecular view of (bdvp)Fe(PMe<sub>3</sub>)<sub>2</sub> (**1-PMe<sub>3</sub>**). Interatomic distances (Å) and angles (°): Fe-N1, 2.057(3); Fe-N2, 2.062(3); Fe-C7, 1.877(3); Fe-C14, 1.888(3); Fe-P1, 2.2285(8); Fe-P2, 2.2280(8); N1-Fe-C7, 81.10(13); N1-Fe-C14, 166.62(13); N1-Fe-N2, 112.43(11); N1-Fe-P1, 89.45(8); N1-Fe-P2, 91.17(8); C7-Fe-C14, 85.61(14); C7-Fe-N2, 166.35(13); C7-Fe-P1, 90.06(10); C7-Fe-P2, 89.61(10); C14-Fe-N2, 80.91(13); C14-Fe-P1, 89.03(9); C14-Fe-P2, 90.26(9); N2-Fe-P1, 91.84(8); N2-Fe-P2, 88.32(8); P1-Fe-P2, 179.24(3).

### Structure of (bdvp)Fe(PMe<sub>3</sub>)<sub>2</sub> (**1-PMe<sub>3</sub>**)

Shown in Fig. 2 is the molecular structure of (bdvp)Fe(PMe<sub>3</sub>)<sub>2</sub> (**1-PMe<sub>3</sub>**), as determined by single crystal X-ray crystallography. The tetradentate ligand essentially resides in a plane of the pseudo-octahedral structure ( $\angle C/N-Fe-P = 90.0(11)^\circ$  (ave);  $\angle P1-Fe-P2 = 179.24(3)^\circ$ ), accompanied by *trans*-PMe<sub>3</sub> groups at  $d(Fe-P) = 2.2283(8)$  Å (ave). The  $d(Fe-N)$  of 2.060(4) (ave) are normal, but there is a splay in the N1-Fe-N2 angle ( $112.43(11)^\circ$ ) indicative of a strain in the chelate. The bite angles of the vinylpyridine are  $81.01(13)^\circ$  (ave), and the phenyl-divinyl bite angle is  $85.61(14)^\circ$ , hence the chelate angles sum to  $360.1^\circ$ .

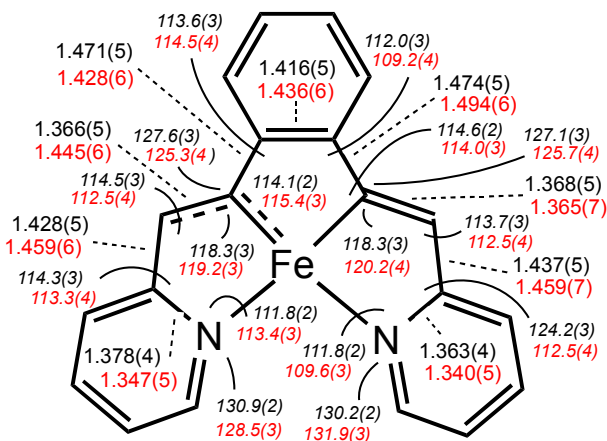
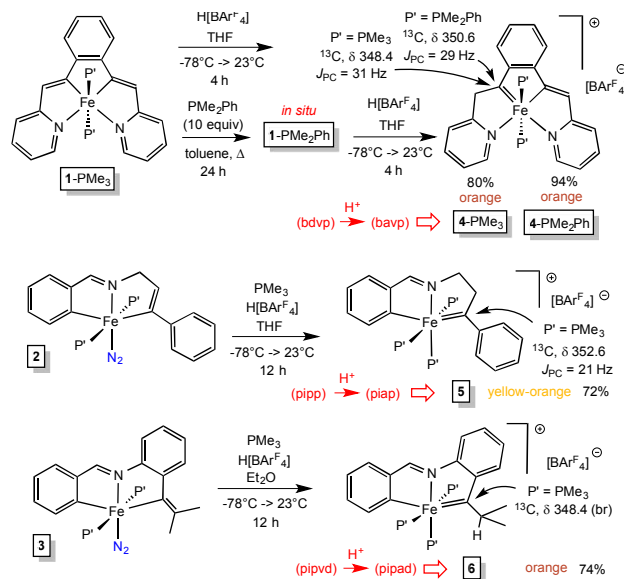


**Fig. 3** Comparative ligand metric parameters (distances (Å), dashed black lines; angles (°, *italics*), curved black lines) for Fe(II) (bdvp)Fe(PMe<sub>3</sub>)<sub>2</sub> (**1-PMe<sub>3</sub>**, black) vs. Fe(IV) [(bavp)Fe(PMe<sub>3</sub>)<sub>2</sub>][BARF<sub>4</sub>] (**4-PMe<sub>3</sub>**, red).

Considerable distortion in the chelate is evident, as the iron-carbon bonds are quite short at  $1.883(8)$  Å (ave), while the C6-C7-C8 and C13-C14-C15 angles of  $127.4(4)$  (ave) deviate significantly from  $120^\circ$ . Fig. 3 illustrates the chelate distances and angles in comparison to those of the related alkylidene complex (*vide infra*). All the angles about the Fe-C bonds are distorted in response to the proximity of the vinyl carbons to the iron. Note

that the pyridines are not perfectly aligned as donors, as the Fe-N-C angles open to an average of  $130.6(5)^\circ$ .



**Scheme 4** Protonations with H[BARF<sub>4</sub>] afford cationic Fe(IV) alkylidenes.

### Vinyl Protonations Lead to Fe(IV) Alkylidenes

The vinyl precursors synthesized via the C-H bond activation and insertion processes were protonated<sup>14-18</sup> to yield cationic Fe(IV) alkylidenes, as illustrated in Scheme 4. Tetradentate chelate complex (bdvp)Fe(PMe<sub>3</sub>)<sub>2</sub> (**1-PMe<sub>3</sub>**) was treated with H[BARF<sub>4</sub>]<sup>30</sup> in THF to afford orange [(bavp)Fe(PMe<sub>3</sub>)<sub>2</sub>][BARF<sub>4</sub>] (**4-PMe<sub>3</sub>**) in 80% yield. The lability of **1-PMe<sub>3</sub>** was tested with excess PMe<sub>2</sub>Ph (10 equiv), and repeated thermolyses in refluxing toluene, including periodic removal of PMe<sub>3</sub>, were required to generate (bdvp)Fe(PMe<sub>2</sub>Ph)<sub>2</sub> (**1-PMe<sub>2</sub>Ph**). Dimethylphenylphosphine derivative **1-PMe<sub>2</sub>Ph** was not isolated, and characterization by NMR spectroscopy proved elusive due to broadened and overlapping resonances. As a consequence, it was generated *in situ* and treated with H[BARF<sub>4</sub>] in THF to yield analytically pure [(bavp)Fe(PMe<sub>2</sub>Ph)<sub>2</sub>][BARF<sub>4</sub>] (**4-PMe<sub>2</sub>Ph**, 94%).

A related protonation of tridentate chelate species *trans*-(pipp)Fe(PMe<sub>3</sub>)<sub>2</sub>N<sub>2</sub> (**2**) in THF initially gave a complex mixture that exhibited a <sup>31</sup>P{<sup>1</sup>H} NMR spectral signature consistent with starting material, a tri-phosphine product, and degradation. The addition of PMe<sub>3</sub> to the reaction resulted in one major product, [(piap)Fe(PMe<sub>3</sub>)<sub>3</sub>][BARF<sub>4</sub>] (**5**) that was isolated as yellow-orange microcrystals in 72% yield. It is likely that an initial dinitrogen-containing Fe(IV) product, [(piap)Fe(PMe<sub>3</sub>)<sub>2</sub>N<sub>2</sub>][BARF<sub>4</sub>], readily loses N<sub>2</sub>, and through redistribution generates **5** along with decomposition products.

Protonation of (pipvd)Fe(PMe<sub>3</sub>)<sub>2</sub>N<sub>2</sub> (**3**) was conducted with H[BARF<sub>4</sub>] in diethyl ether, and a mixture spectrally related to that of the initial protonation of **2** was discerned. Again, the addition of PMe<sub>3</sub> to the reaction mixture permitted the isolation of [(pipvd)Fe(PMe<sub>3</sub>)<sub>3</sub>][BARF<sub>4</sub>] (**6**) in 74% yield as orange microcrystals.

Definitive spectral characterization of the isolated Fe(IV) alkylidene complexes was predicated on observation of diagnostic downfield <sup>13</sup>C resonances<sup>31,32</sup> attributed to M=CRR' functionality (Scheme 4). The spectral signatures were difficult to

detect, requiring indirect methods, but the alkylidene values for **4-PMe<sub>3</sub>**, **4-PMe<sub>2</sub>Ph**, **5**, and **6** were eventually observed at  $\delta$  348.4 ( $J_{PC} = 31$  Hz),  $\delta$  350.6 ( $J_{PC} = 31$  Hz),  $\delta$  352.6 ( $J_{PC} = 21$  Hz), and  $\delta$  348.4 (br), respectively.

5

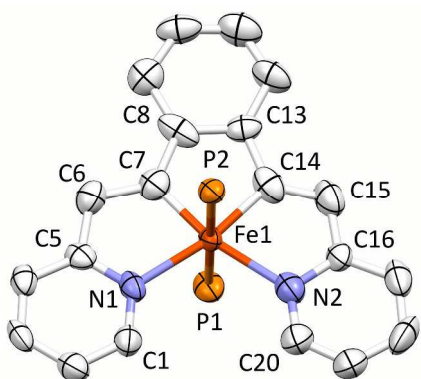


**Fig. 4.** Molecular view of the cation pertaining to [(bavp)Fe(PMe<sub>3</sub>)<sub>2</sub>][BARF<sub>4</sub>] (**4-PMe<sub>3</sub>**); the PMe<sub>3</sub> methyl groups have been removed for clarity. Interatomic distances (Å) and angles (°): Fe-N1, 2.083(3); Fe-N2, 2.129 (4); Fe-C7, 1.809(4); Fe-C14, 1.858(4); Fe-P1, 2.2671(11); Fe-P2, 2.2725(11); N1-Fe-C7, 81.47(17); N1-Fe-C14, 168.31(19); N1-Fe-N2, 110.98(14); N1-Fe-P1, 88.53(9); N1-Fe-P2, 91.32(9); C7-Fe-C14, 86.9(2); N2-Fe-C7, 167.48(17); C7-Fe-P1, 91.87(13); C7-Fe-P2, 87.81(13); N2-Fe-C14, 80.71(18); C14-Fe-P1, 91.49(13); C14-Fe-P2, 88.60(13); N2-Fe-P1, 89.89(10); N2-Fe-P2, 90.44(10); P1-Fe-P2, 179.66(5).

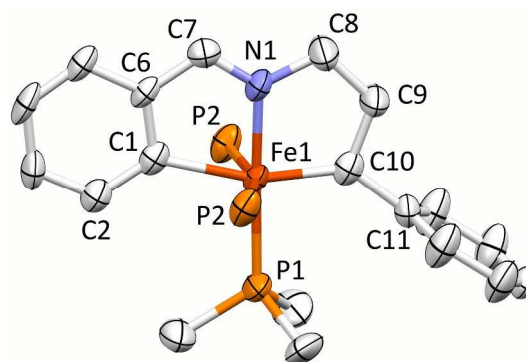
#### Structure of [(bavp)Fe(PMe<sub>3</sub>)<sub>2</sub>][BARF<sub>4</sub>] (**4-PMe<sub>3</sub>**)

A molecular view of the cation pertaining to [(bavp)Fe(PMe<sub>3</sub>)<sub>2</sub>][BARF<sub>4</sub>] (**4-PMe<sub>3</sub>**) is illustrated in Fig 4, and it shows its distorted octahedral structure, with the tetradentate chelate occupying a single plane. The P-Fe-C/N angles average 90.0(15)°, and there is a splay in the bavp ligand indicated by the N1-Fe-N2 angle of 110.98(14), and the *trans*-N-Fe-C angles of 168.31(19) and 167.48(17)°.

The critical  $d(\text{Fe}=\text{C}7)$  is 1.809(4) Å, which is ~0.05 Å shorter than the adjacent iron-vinyl carbon distance of 1.858(4) Å. Both are shorter than the iron-carbon bond lengths in **1-PMe<sub>3</sub>**, in contrast to the  $d(\text{Fe}-\text{N})$ , which are longer at 2.083(3) and 2.129(4) Å. As these changes and the comparison between **1-PMe<sub>3</sub>** and **4-PMe<sub>3</sub>** in Fig. 3 reveal, the chelate has pinched in to a slightly greater extent in the cation. Angles C6-C7-C8 and C13-C14-C15 are 2.3 and 1.4° less than the corresponding angles in **1-PMe<sub>3</sub>**, and the remaining chelate distances and angles change in concert.

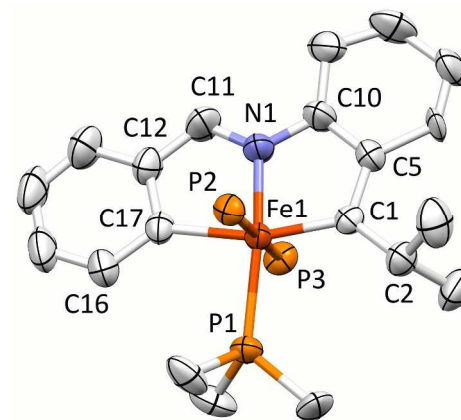
#### Structure of [(piap)Fe(PMe<sub>3</sub>)<sub>3</sub>][BARF<sub>4</sub>] (**5**)

Fig 5 displays a molecular view of the cation corresponding to [(piap)Fe(PMe<sub>3</sub>)<sub>3</sub>][BARF<sub>4</sub>] (**5**), and reveals its pseudo-octahedral geometry with the piap ligand occupying a *mer*-configuration about iron. The critical alkylidene distance,  $d(\text{Fe}-\text{C}10)$  is 1.867(7) Å, which is significantly shorter than  $d(\text{Fe}-\text{C}1) = 2.106(6)$  Å, but on par with the iron-vinyl carbon distances in **1-PMe<sub>3</sub>** (1.883(8) Å (ave)) and **4-PMe<sub>3</sub>** (1.858(4) Å). The tridentate chelate is strained, as the C1-Fe-C10 angle is 161.6(3)°, and the Fe-C10-C9 and Fe-C10-C11 angles of 115.7(5)° and 136.4(5)°, respectively, indicate that the alkylidene is not perfectly oriented. Note that the C10-Fe-P2 angles are 100.20(4)°; as a consequence, the d-orbital that comprises the iron portion of the Fe=C  $\pi$ -bond has some Fe-P  $\sigma^*$  character that aids in producing better overlap with the carbon p-orbital.



55

**Fig. 5.** Molecular view of the cation pertaining to [(piap)Fe(PMe<sub>3</sub>)<sub>3</sub>][BARF<sub>4</sub>] (**5**); the methyl groups of the *trans*-PMe<sub>3</sub> ligands have been removed for clarity. Interatomic distances (Å) and angles (°): Fe-C1, 2.106(6); Fe-N1, 1.949(6); Fe-C10, 1.867(7); Fe-P1, 2.281(2); Fe-P2, 2.2733(16); C7-N1, 1.307(9); C1-Fe-N1, 78.4(3); C1-Fe-C10, 161.6(3); C1-Fe-P1, 103.7(2); N1-Fe-C10, 83.2(3); N1-Fe-P1, 177.94(17); C10-Fe-P1, 94.8(2); C1-Fe-P2, 79.47(4); N1-Fe-P2, 88.54(5); C10-Fe-P2, 100.20(4); P1-Fe-P2, 91.83(5); P2-Fe-P2, 158.89(8); Fe-C1-C2, 133.8(5); Fe-C1-C6, 110.4(5); Fe-C10-C9, 115.7(5); Fe-C10-C11, 136.4(5).



**Fig. 6.** Molecular view of the cation pertaining to [(pipad)Fe(PMe<sub>3</sub>)<sub>3</sub>][BARF<sub>4</sub>] (**6**); the methyl groups of the *trans*-PMe<sub>3</sub> ligands have been removed for clarity. Interatomic distances (Å) and angles (°): Fe-C1, 1.899(3); Fe-N1, 1.933(3); Fe-C17, 2.059(3); Fe-P1, 2.317(2); Fe-P2, 2.226(3); Fe-P3, 2.367(3); N1-C11, 1.307(5); C1-C2, 1.525(5); N1-Fe-C17, 80.04(14); C1-Fe-C17, 163.36(15); C17-Fe-P1, 92.03(12); C17-Fe-P2, 88.28(13); C17-Fe-P3, 87.16(12); N1-Fe-C1, 83.34(14); N1-Fe-P1, 167.04(14); N1-Fe-P2, 96.52(16); N1-Fe-P3, 79.34(14); C1-Fe-P1, 104.46(12); C1-Fe-P2, 92.87(12); C1-Fe-P3, 90.53(13); P1-Fe-P2, 93.45(14); P1-Fe-P3, 90.11(13); P2-Fe-P3, 174.32(13); Fe-C17-C16, 136.0(3); Fe-C17-C12, 110.8(3); Fe-C1-C5, 112.8(2); Fe-C1-C2, 131.0(3).

#### Structure of [(pipad)Fe(PMe<sub>3</sub>)<sub>3</sub>][BARF<sub>4</sub>] (**6**)

A molecular view of the cation of [(pipad)Fe(PMe<sub>3</sub>)<sub>3</sub>][BARF<sub>4</sub>] (**6**) is provided in Fig. 6, which indicates the *mer*-octahedral structure of the iron alkylidene. The tridentate pipad chelate is essentially planar, and the isopropyl-aryl alkylidene possesses a  $d(\text{Fe}=\text{C})$  of 1.899(3) Å, a value longer than the iron-vinyl carbon distances in **1-PMe<sub>3</sub>** and **4-PMe<sub>3</sub>**. Again, the chelate exhibits strain about the core, as the C1-Fe-C17 angle is 163.36(15)°, and its isopropyl group exerts a steric influence on the unique PMe<sub>3</sub>, as the C1-Fe-P1 angle is 104.46(12)°. The Fe-C1-C5 and Fe-C1-C2 angles are 112.8(2)° and 131.0(3)°, respectively, showing that the alkylidene

is at an imperfect orientation with respect to the iron.

### Structural Comparisons

In Table 1., a comparison of known Fe(IV) alkylidenes is given in reference to  $d(\text{Fe}=\text{C})$  and  $^{13}\text{C}$  NMR chemical shift ( $\delta$ ).<sup>29,30</sup> Paramagnetic derivatives are on the long side of the bond distance values, and the electronic structure analysis by Chirik *et al.*<sup>13</sup> of the PDI derivatives suggests that these species are best considered carbene radicals.<sup>33</sup> The  $\pi$ -interaction is construed as a carbene radical antiferromagnetically (AF) coupled to a metal  $d\pi$ -electron of appropriate symmetry. Modern calculations have not been employed on Floriani's calix[4]arane diphenylcarbene complexes,<sup>17</sup> but they are high spin, and therefore likely to conform to an AF coupling model.

Of the remaining diamagnetic complexes, some relative distances appear to be a clear consequence of the *trans*-influence. When no ligand is opposite the diphenylcarbene, the distance is short, as in the cases of  $(\text{tmtaa})\text{Fe}=\text{CPh}_2$  (**B**)<sup>10</sup> and  $(\text{TPFPP})\text{Fe}=\text{CPh}_2$  (**A**).<sup>12</sup> As the methylimidazole adduct of the latter (i.e.,  $(\text{TPFPP})\text{Fe}(\text{CPh}_2)(\text{MeIm})$  (**A**))<sup>12</sup> indicates, the distance is increased by 0.55 Å. It is not surprising that the complexes herein have  $d(\text{Fe}=\text{C})$  that range from 1.809–1.899 Å, given the presence of a strong *trans*-influence ligand, an aryl. There is no straightforward correlation of  $d(\text{Fe}=\text{C})$  to its respective  $^{13}\text{C}$  NMR spectroscopic shift.

**Table 1.** Comparison of Iron-alkylidene  $d(\text{Fe}=\text{C})$  and  $^{13}\text{C}$  NMR shift ( $\delta$ ).

30 Cmpd <sup>a</sup>	$d(\text{Fe}=\text{C})$ (Å)	$\delta$ ( $^{13}\text{C}=\text{Fe}$ )
$(\text{tmtaa})\text{Fe}=\text{CPh}_2$ ( <b>B</b> ) <sup>b</sup>	1.794(3)	313.2
$(\text{TPFPP})\text{Fe}=\text{CPh}_2$ ( <b>A</b> ) <sup>c</sup>	1.767(3)	359.0
$[\text{Cp}^*(\text{dppe})\text{Fe}=\text{CH}(\text{Me})]\text{PF}_6$ ( <b>E</b> ) <sup>d</sup>	1.787(8)	336.6
35 $[(\text{bavp})\text{Fe}(\text{PMe}_3)_2][\text{BAR}^{\text{F}}_4]$ ( <b>4-PMe}_3</b> )	1.809(4)	350.6
$(\text{TPFPP})\text{Fe}(\text{CPh}_2)(\text{MeIm})$ ( <b>A</b> ) <sup>c</sup>	1.827(5)	385.4
$[(\text{piap})\text{Fe}(\text{PMe}_3)_3][\text{BAR}^{\text{F}}_4]$ ( <b>5</b> )	1.867(7)	352.6
$[(\text{pipad})\text{Fe}(\text{PMe}_3)_3][\text{BAR}^{\text{F}}_4]$ ( <b>6</b> )	1.899(3)	348.4
$(^{\text{Et}}\text{PDI})\text{Fe}=\text{CPh}_2$ ( <b>C</b> ) <sup>e</sup>	1.9205(19)	para
40 $(^{\text{Me}}\text{EtPDI})\text{Fe}=\text{CPh}_2$ ( <b>C</b> ) <sup>e</sup>	1.9234(18)	para
	1.9357(18)	para
$[p\text{-Bu-calix}[4](\text{O})_2(\text{OMe})_2]\text{Fe}=\text{CPh}_2$ ( <b>D</b> ) <sup>f</sup>	1.943(8)	para
$[p\text{-Bu-calix}[4](\text{O})_2(\text{OSiMe}_3)_2]\text{Fe}=\text{CPh}_2$ ( <b>D</b> ) <sup>f</sup>	1.958(5)	para
	1.973(5)	para

<sup>a</sup>See Fig. 1 for ligand structural types corresponding to **A–D**. <sup>b</sup>Ref. 10. <sup>c</sup>Ref. 12. <sup>d</sup>Ref. 9. <sup>e</sup>Ref. 13. <sup>f</sup>Ref. 11.

### Mössbauer Analysis of Fe(II) and Fe(IV) Chelates

Shown in Fig. 7 are Mössbauer spectra of the related Fe(II) and Fe(IV) complexes *trans*-(pipvd)Fe(PMe<sub>3</sub>)<sub>2</sub>N<sub>2</sub> (**3**) and  $[(\text{pipad})\text{Fe}(\text{PMe}_3)_3][\text{BAR}^{\text{F}}_4]$  (**6**), respectively. In Table 2, all Mössbauer parameters for corresponding Fe(II) and Fe(IV) compounds are listed. The data in Table 2 reveal isomer shifts for the diamagnetic species all within  $\Delta\delta$  of 0.1 mm/s, and provide a textbook example of why they should not be simply correlated with formal oxidation state, but are strong indicators of covalency.<sup>34,35</sup> "Iron-ligand bond lengths play a decisive role for the isomer shift of a compound",<sup>35</sup> and the data in Table 2, and Figs. 2–4 bear this out. Minimal bond distance changes occur in the protonation of  $(\text{bdvp})\text{Fe}(\text{PMe}_3)_2$  (**1-PMe}\_3**) to afford  $[(\text{bavp})\text{Fe}(\text{PMe}_3)_2][\text{BAR}^{\text{F}}_4]$  (**4-PMe}\_3**), and similarly small  $d(\text{Fe}-\text{L}/\text{X})$  changes are likely in the related protonations, leading to small isomer shift differences.

One counter argument regarding interpretation of isomer shifts pertains to the somewhat arbitrary formalism of treating a

Schrock alkylidene as a (2-) ligand, whereas a Fischer carbene, in which conjugated lone pairs can donate to the carbon (i.e.,  $\text{M}=\text{C}(\text{R}) \leftrightarrow \text{M}^{(-)}-\text{C}=\text{X}^{(+)}(\text{R})$ ), is neutral. While one can argue some conjugation for **3** and **6**, the other cases are less readily interpreted in this fashion, especially given the orientation of the

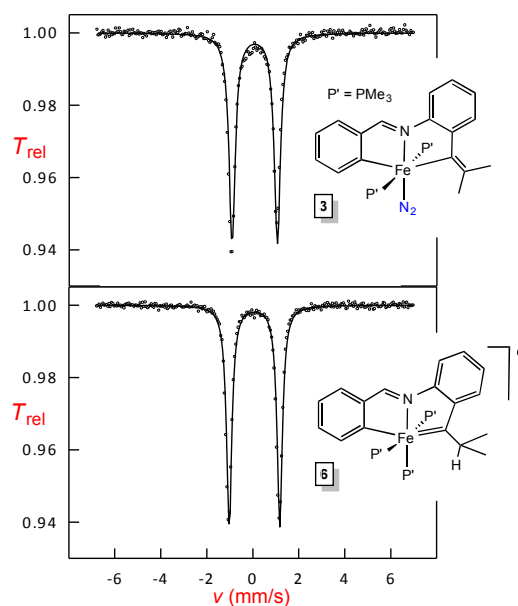


**Fig. 7.** Mössbauer spectra of Fe(II) *trans*-(pipvd)Fe(PMe<sub>3</sub>)<sub>2</sub>N<sub>2</sub> (**3**,  $\delta = 0.07(1)$  mm/s;  $\Delta E_Q = 1.97(1)$  mm/s), and the corresponding Fe(IV) cation  $[(\text{pipad})\text{Fe}(\text{PMe}_3)_3][\text{BAR}^{\text{F}}_4]$  (**6**,  $\delta = 0.07(1)$  mm/s;  $\Delta E_Q = 2.20(1)$  mm/s).

phenyl group of **5** as roughly orthogonal to the Fe=C interaction. There can be little question that two pairs of electrons -- one sigma and one pi -- exist between iron and carbon in these compounds, and that the parameters of the Mössbauer spectra correlate with a strong degree of covalency. Previously characterized alkylidene species are limited to Chirik *et al.*,<sup>13</sup> whose  $S = 1$  systems are sufficiently different to be essentially incomparable.

**Table 2.** Comparison of Fe(II) and Fe(IV) alkylidene Mössbauer parameters.

90 Cmpd	$\delta$ (mm/s)	$\Delta E_Q$ (mm/s)	$\Gamma_{\text{FWHM}}$ (mm/s)
$(\text{bdvp})\text{Fe}(\text{PMe}_3)_2$ ( <b>1-PMe}_3</b> )	0.09(1)	1.96(1)	0.45(1)
<i>trans</i> -(pipp)Fe(PMe <sub>3</sub> ) <sub>2</sub> N <sub>2</sub> ( <b>2</b> ) <sup>a</sup>	0.08(1)	2.14(1)	0.31(1)
<i>trans</i> -(pipvd)Fe(PMe <sub>3</sub> ) <sub>2</sub> N <sub>2</sub> ( <b>3</b> )	0.07(1)	1.97(1)	0.33(1)
95 $[(\text{bavp})\text{Fe}(\text{PMe}_3)_2][\text{BAR}^{\text{F}}_4]$ ( <b>4-PMe}_3</b> ) <sup>b</sup>	0.01(1)	2.67(1)	0.28(1)
$[(\text{piap})\text{Fe}(\text{PMe}_3)_3][\text{BAR}^{\text{F}}_4]$ ( <b>5</b> ) <sup>c</sup>	0.06(1)	2.02(1)	0.29(1)
$[(\text{pipad})\text{Fe}(\text{PMe}_3)_3][\text{BAR}^{\text{F}}_4]$ ( <b>6</b> )	0.07(1)	2.20(1)	0.28(1)

<sup>a</sup>Sample contained 20% of a high spin Fe(II) species:  $\delta = 1.23(1)$  mm/s,  $\Delta E_Q = 2.40(1)$  mm/s,  $\Gamma_{\text{FWHM}} = 0.73(1)$  mm/s. <sup>b</sup>Sample contained 18% of a high spin Fe(II) species:  $\delta = 1.28(1)$  mm/s,  $\Delta E_Q = 2.70(1)$  mm/s,  $\Gamma_{\text{FWHM}} = 0.54(1)$  mm/s. <sup>c</sup>Sample contained 35% of a high spin Fe(II) species:  $\delta = 1.25(1)$  mm/s,  $\Delta E_Q = 2.42(1)$  mm/s,  $\Gamma_{\text{FWHM}} = 0.51(1)$  mm/s.

Interpretation of the quadrupole splitting ( $\Delta E_Q$ ), a measure of the electric field gradient at the nucleus,<sup>35</sup> is less transparent. The changes in ligand coordination, principally PMe<sub>3</sub> for N<sub>2</sub> in the conversion of **2** and **3** to **5** and **6**, respectively, are apparently significant enough to offset changes to the Ar-Fe-(V)y/=C) axes. For **1-PMe}\_3** and **4-PMe}\_3**, there is a consequential change from

$\Delta E_Q = 1.96(1)$  mm/s to  $2.67(1)$  mm/s, as the rhombicity of the complex is notably altered due to the change from a symmetric divinyl coordination to that of the alkylidene and vinyl arrangement.

## Conclusions

Protonation of Fe(II) chelate complexes in which iron-vinyl bonds are present led to the formation of four cationic Fe(IV) alkylidene complexes, three of which are structurally characterized. Prior to this study,  $[\text{Cp}^*(\text{dppe})\text{Fe}=\text{CH}(\text{Me})]\text{PF}_6$  was the only non-aryl Fe(IV) alkylidene that had undergone X-ray structural analysis, although numerous related  $[\text{CpLL}'\text{Fe}=\text{CHR}]^+$  have been synthesized.<sup>7-9,14-16</sup>

This study confers confidence in iron-vinyl protonation as a viable, general route to Fe(IV) alkylidenes in non-Cp systems. The compounds herein (i.e., **4**-PMe<sub>3</sub>, **5**, **6**) were not active towards metathesis (e.g., *cis*-2-pentene, RCCR, R = Me, Ph) or cyclopropanation, primarily because PMe<sub>3</sub> is not sufficiently labile, as expected. In order to implement this route toward viable olefin metathesis catalysts, future syntheses must address three factors: 1) complexes must be coordinatively unsaturated, with 14e<sup>-</sup> species the obvious targets based on ruthenium analogues; 2) complexes must be neutral or anionic, where the d-orbitals are less contracted; and 3) Fe=CHR moieties must be targeted.

## Experimental Section

Experimental details, full spectral characterizations, and a description of the Mössbauer spectroscopic analysis are given in the Supplemental Information. For general descriptions, consult the Schemes. Some crystallographic information is given below.

*Crystal data for 1*-PMe<sub>3</sub>: C<sub>26</sub>H<sub>32</sub>N<sub>2</sub>P<sub>2</sub>Fe, *M* = 490.33, triclinic, *P*-1, *a* = 10.2138(8), *b* = 10.6014(8), *c* = 12.4208(10) Å,  $\alpha$  = 88.674(4)°  $\beta$  = 67.062(3)°  $\gamma$  = 89.687(4)°, *V* = 1238.24(17) Å<sup>3</sup>, *T* = 203(2),  $\lambda$  = 0.71073 Å, *Z* = 2, *R*<sub>int</sub> = 0.0311, 22420 reflections, 6098 independent, *R*<sub>1</sub>(all data) = 0.0663, *wR*<sub>2</sub> = 0.1766, GOF = 1.077, CCDC-1057831.

*Crystal data for 4*-PMe<sub>3</sub>: C<sub>58</sub>H<sub>45</sub>N<sub>2</sub>F<sub>24</sub>BP<sub>2</sub>Fe, *M* = 1354.56, monoclinic, *P*<sub>2</sub>/c, *a* = 19.6517(7), *b* = 12.5655(4), *c* = 25.3645(7) Å,  $\beta$  = 109.7450(10)°, *V* = 5895.1(3) Å<sup>3</sup>, *T* = 203(2),  $\lambda$  = 0.71073 Å, *Z* = 4, *R*<sub>int</sub> = 0.0365, 49817 reflections, 12059 independent, *R*<sub>1</sub>(all data) = 0.0958, *wR*<sub>2</sub> = 0.1782, GOF = 1.012, CCDC-1057830.

*Crystal data for 5*(THF): C<sub>61</sub>H<sub>60</sub>NOF<sub>24</sub>BP<sub>3</sub>Fe, *M* = 1438.67, monoclinic, *C*2/m, *a* = 19.963(5), *b* = 17.492(6), *c* = 19.586(6) Å,  $\beta$  = 93.869(14)°, *V* = 6824(4) Å<sup>3</sup>, *T* = 203(2),  $\lambda$  = 0.71073 Å, *Z* = 4, *R*<sub>int</sub> = 0.0579, 21278 reflections, 5076 independent, *R*<sub>1</sub>(all data) = 0.0899, *wR*<sub>2</sub> = 0.1923, GOF = 1.155, CCDC-1057829.

*Crystal data for 6*: C<sub>58</sub>H<sub>55</sub>NF<sub>24</sub>BP<sub>3</sub>Fe, *M* = 1381.60, monoclinic, *P*<sub>2</sub>/c, *a* = 18.4232(6), *b* = 13.0618(4), *c* = 25.9802(8) Å,  $\beta$  = 99.5300(10)°, *V* = 6165.6(3) Å<sup>3</sup>, *T* = 233(2),  $\lambda$  = 0.71073 Å, *Z* = 4, *R*<sub>int</sub> = 0.0393, 35706 reflections, 9178 independent, *R*<sub>1</sub>(all data) = 0.0780, *wR*<sub>2</sub> = 0.1273, GOF = 1.050, CCDC-1057828.

## Acknowledgements

Support from the National Science Foundation (1402149), Cornell University, and Friedrich Alexander University, is gratefully acknowledged.

## Notes and references

<sup>a</sup>Department of Chemistry & Chemical Biology, Baker Laboratory, Cornell University, Ithaca, NY, 14850, USA. Fax: 607 255 4137; Tel: 607 255 7220; E-mail: ptw2@cornell.edu

<sup>b</sup>Department of Chemistry & Pharmacy, Friedrich Alexander University Erlangen-Nürnberg (FAU), Egerlandstr. 1, D-91058 Erlangen, Germany

† Electronic Supplementary Information (ESI) available: CCDC-1057828-31. See DOI:

- H. Jeong, J. M. John, R. R. Schrock, A. H. Hoveyda, *J. Am. Chem. Soc.*, 2015, **137**, 2239-2242.
- (a) R. R. Schrock, *Angew. Chem. Int. Ed.*, 2006, **45**, 3748-3759. (b) R. R. Schrock, A. H. Hoveyda, *Angew. Chem. Int. Ed.*, 2003, **42**, 4592-4633.
- V. M. Marx, A. H. Sullivan, M. Melaimi, S. C. Virgil, B. K. Keitz, D. S. Weinberger, G. Bertrand, R. H. Grubbs, *Angew. Chem. Int. Ed.*, 2015, **54**, 1919-1923.
- Grubbs, R. H., *Angew. Chem. Int. Ed.*, 2006, **45**, 3760-3765.
- Y. Chauvin, *Angew. Chem. Int. Ed.*, 2006, **45**, 3740-3747.
- O. Eisenstein, R. Hoffmann, A. R. Rossi, *J. Am. Chem. Soc.*, 1981, **103**, 5582-5584.
- (a) M. Brookhart, J. R. Tucker, G. R. Husk, *J. Am. Chem. Soc.*, 1983, **105**, 258-264. (b) M. Brookhart, J. R. Tucker, *J. Am. Chem. Soc.*, 1981, **103**, 979-981. (c) M. Brookhart, D. Timmers, J. R. Tucker, G. D. Williams, G. R. Husk, H. Brunner, B. Hammer, *J. Am. Chem. Soc.*, 1983, **105**, 6721-6723.
- G. Poignant, S. Nlate, V. Guerschais, A. J. Edwards, P. R. Raithby, *Organometallics*, 1997, **16**, 124-132.
- V. Mahias, S. Cron, L. Toupet, C. Lapinte, *Organometallics*, 1996, **15**, 5399-5408.
- A. Klose, E. Solari, C. Floriani, N. Re, A. Chiesi-Villa, C. Rizzoli, *Chem. Commun.*, 1997, 2297-2298.
- V. Esposito, E. Solari, C. Floriani, N. Re, C. Rizzoli, A. Chiesi-Villa, *Inorg. Chem.*, 2000, **39**, 2604-2613.
- Y. Li, J.-S. Huang, Z.-Y. Zhou, C.-M. Che, X.-Z. You, *J. Am. Chem. Soc.*, 2002, **124**, 13185-13193.
- S. K. Russell, J. M. Hoyt, S. C. Bart, C. Milsman, S. C. E. Stieber, S. P. Sempronio, S. DeBeer, P. J. Chirik, *Chem Sci.*, 2014, **5**, 1168-1174.
- (a) K. A. M. Kremer, G.-H. Kuo, E. J. O'Connor, P. Helquist, R. C. Kerber, *J. Am. Chem. Soc.*, 1982, **104**, 6119-6121. (b) G.-H. Kuo, P. Helquist, R. C. Kerber, *Organometallics*, 1984, **3**, 806-808.
- T. Bodnar, A. R. Cutler, *J. Organomet. Chem.*, 1981, **213**, C31-C36.
- (a) A. Davison, J. P. Selegue, *J. Am. Chem. Soc.*, 1978, **100**, 7763-7765. (b) R. D. Adams, A. Davison, J. P. Selegue, *J. Am. Chem. Soc.*, 1979, **101**, 7232-7238.
- M. I. Bruce, A. G. Swincer, *Aust. J. Chem.*, 1980, **33**, 1471-1483.
- C. P. Casey, W. H. Miles, H. Tukada, J. M. O'Connor, *J. Am. Chem. Soc.*, 1982, **104**, 3761-3762.
- H. H. Karsch, *Chem. Ber.*, 1977, **110**, 2699-2711.
- (a) G. Xu, H. Sun, X. Li, *Organometallics*, 2009, **28**, 6090-6095. (b) X. Xu, J. Jia, H. Sun, Y. Liu, W. Xu, Y. Shi, D. Zhang, X. Li, *Dalton Trans.*, 2013, **42**, 3417-3428.
- (a) R. Beck, T. Zheng, H. Sun, X. Li, U. Flörke, H.-F. Klein, *J. Organomet. Chem.*, 2008, **693**, 3471-3478. (b) S. Camadanli, R. Beck, U. Flörke, H.-F. Klein, *Organometallics*, 2009, **28**, 2300-2310. (c) H.-F. Klein, S. Camadanli, R. Beck, D. Leukel, U. Flörke, *Angew. Chem. Int. Ed.*, 2005, **44**, 975-977. (d) H.-F. Klein, S. Camadanli, R. Beck, U. Flörke, *Chem. Commun.*, 2005, 381-382.
- E. C. Volpe, P. T. Wolczanski, E. B. Lobkovsky, *Organometallics*, 2010, **29**, 364-377.
- E. R. Bartholomew, E. C. Volpe, P. T. Wolczanski, E. B. Lobkovsky, T. R. Cundari, *J. Am. Chem. Soc.*, 2013, **135**, 3511-3527.
- T. Yamamori, K. Nagata, N. Ishizuka, K. Hayashi, "Utilities of Olefin Derivatives", US Patent Appl. No. 10/489,365, 2004.
- Rodrigues, N.; Bennis, K.; Vivier, D.; Pereira, V.; C. Chatelain, F.; Chapuy, E.; Deokar, H.; Busserolles, J.; Lesage, F.; Eschalier, A.; Ducki, S. *Eur. J. Med. Chem.* **2014**, **75**, 391-402.
- G. Wolf, E.-U. Würthwein, *Chemische Berichte*, 1991, **124**, 655-663.

- 27 (a) C. Shi, Q. Zhang, K. K. Wang, *J. Org. Chem.*, 1999, **64**, 925-932.  
(b) H. Kusama, J. Takaya, N. Iwasawa, *J. Am. Chem. Soc.*, 2002, **124**, 11592-11593.
- 28 J. L. Crossland, D. R. Tyler, *Coord. Chem. Rev.*, 2010, **254**, 1883-1894.
- 5 29 N. Hazari, *Chem. Soc. Rev.*, 2010, **39**, 4044-4056.
- 30 M. Brookhart, B. Grant, A. F. Volpe, Jr., *Organometallics*, 1992, **11**, 3920-3922.
- 31 J. Louie, R. H. Grubbs, *Organometallics*, 2002, **21**, 2153-2164.
- 10 32 J. Feldman, R. R. Schrock, in *Prog. Inorg. Chem.*, Vol 39, S. J. Lippard, Ed.; Wiley and Sons: New York, 1991, pp 1-74.
- 33 W. I. Dzik, X. P. Zhang, B. de Bruin, *Inorg. Chem.*, 2011, **50**, 9896-9903.
- 34 F. Neese, *Inorg. Chim Acta*, 2002, **337**, 181-192.
- 15 35 P. Gütllich, E. Bill, A. X. Trautwein, *Mössbauer Spectroscopy and Transition Metal Chemistry: Fundamentals and Applications*; Springer-Verlag: Berlin, 2011.

20